Path instability of rising spheroidal air bubbles: A shape-controlled process

Roberto Zenit[1] and Jacques Magnaudet[2]
[1]*Instituto de Investigaciones en Materiales, Universidad Nacional Autónoma de México, Apdo. Postal 70-360, México D.F. 04510, Mexico*
[2]*Institut de Mécanique des Fluides de Toulouse, Allée du Professeur Camille Soula, 31400 Toulouse, France*

(Received 27 March 2008; accepted 16 May 2008; published online 25 June 2008)

The conditions for which the paths of freely rising bubbles become oscillatory are studied experimentally using silicone oils with viscosities ranging from 0.5 to 9.4 times that of water. Since these fluids are nonpolar, as opposed to water, the gas-liquid interfaces remain clean without the need of an ultrapure environment. We find the Reynolds number at incipient transition to vary from 70 to 470, for decreasing liquid viscosity. Correspondingly, the bubble aspect ratio remains almost constant, ranging only from 2.36 to 2.0 for the same set of conditions. Hence, we argue that the dominant parameter to trigger the instability is the bubble shape and not the Reynolds number. Since vorticity generated at the bubble surface is almost independent of the Reynolds number and mostly depends on the bubble aspect ratio in the parameter range covered by our experiments, present results strongly support the view that path instability is a direct consequence of the wake instability that occurs when this surface vorticity exceeds a certain threshold. © *2008 American Institute of Physics*. [DOI: 10.1063/1.2940368]

Air bubbles larger than a certain size rising in water under the effect of buoyancy are known to follow paths with horizontal oscillations, while they are only submitted to a vertical gravitational force. This paradigm has caught the attention of scientists for centuries, starting with Leonardo da Vinci's observations.[1] Rigorous studies of the phenomenon were conducted over the last 50 years. In water, small bubbles (say, less than 1.5 mm in diameter) are kept almost spherical by surface tension and rise along a straight path, while slightly larger bubbles follow a zigzag or a helical path. Until recently the reasons for this change of behavior, as well as the precise threshold at which it occurs, remained unclear. Early experiments conducted in water, under apparently the same conditions, gave a broad range of conditions for the transition to oscillatory path to occur (see Ref. 2 for a review). The experimental results of Duineveld[3] obtained in hyperclean water gave a new insight into the phenomenon, as they made it clear that in most of the previous experiments the air-water system contained some surfactants which prevented the interface from being stress-free, changing the dynamics of the problem completely.

The nature of the path instability was first investigated theoretically by considering the possibility of an irrotational mechanism.[4,5] This view was, however, shown to be incorrect both by a rigorous numerical stability analysis[6] and by experiments.[7] Only recently, through direct numerical simulations of the Navier–Stokes equations around a freely moving spheroidal bubble with a prescribed shape, has the nature of the instability began to be understood.[8] In this model, the trajectory becomes unstable as a result of an instability of the wake. In particular, the onset of path instability was found to coincide with the time at which the wake loses its axial symmetry and develops two counter-rotating trailing vortices,[8] an observation confirmed by experiments in hyperclean water.[9] The first indication of the relation between wake instability and bubble path was reported by Brücker.[10]

Of particular relevance to this study is the work of Magnaudet and Mougin[11] who performed numerical simulations of the flow past a fixed oblate spheroidal bubble of prescribed shape embedded in a uniform stream to determine the range of parameters for which the wake becomes unstable. They found that this cannot occur whatever the Reynolds number for bubbles with an aspect ratio χ less than 2.21, while for higher χ the wake experiences a steady supercritical bifurcation for a critical Reynolds number decreasing as χ increases. Since the vorticity generated at the bubble surface owing to the stress-free condition is at the root of the mechanism, they built a criterion to determine whether the flow is unstable or not, based on the maximum of this quantity. Although the nature of the instability affecting the wake of a *fixed* bubble is now clearer (see also Ref. 12), the experimental evidence to further support the applicability of these ideas to *freely rising* bubbles is still limited. This is partly because there are only a few experimental results for hyperclean water[3,9,13] and, to our knowledge, "clean" experiments with other liquids have not been carried out.

In this letter we report new experimental results which clarify the conditions for the transition to an oscillatory path for the case of clean fluids different from water, namely, silicone oils. As is well known, these fluids are formed by nonpolar molecules as opposed to water. This feature makes the gas-liquid interfaces remain clean under standard laboratory conditions. Our experiments make use of several silicone oils with viscosities ranging from half that of water to ten times this value. The most important result of this inves-

TABLE I. Properties of the liquids used in the experiment: ρ is the density, μ the dynamic viscosity, and σ the surface tension. The properties of pure water are also shown for reference.

Liquid	ρ (kg/m^3)	μ (mPa s)	σ (mN/m)	Mo$=g\mu^4/(\rho\sigma^3)$
Water	1000	1.00	72.86	2.5×10^{-11}
DMS-T00	761	0.49	15.9	1.8×10^{-10}
DMS-T02	873	1.75	18.7	1.6×10^{-8}
DMS-T05	918	4.59	19.7	6.2×10^{-7}
DMS-T11	935	9.35	20.1	9.9×10^{-6}

tigation is that, when the liquid viscosity is varied, the conditions for transition to an oscillating path occur over a wide range of values of the Reynolds number while the critical aspect ratio remains mostly unchanged.

The experiments were conducted in a 30 cm tall cylindrical glass tank, with a 10 cm diameter. At the bottom of the container a capillary tube within which the bubbles were formed was inserted. Bubbles of different sizes were produced by changing the diameter of the capillary and also by lightly tapping the tubing (to add a small disturbance to the gas flow). The bubbles were formed with air which was injected in the capillary tube using a syringe pump. By using very small pumping rates (1 μl/min), the formation of single bubbles was made possible. To ensure that the interfaces remained clean, all parts in direct contact with the liquid (glass container and capillaries) were thoroughly cleaned before each experiment: They were rinsed twice with methanol (Aldrich, 27047-4, 99.9% purity) and four times with double-distilled water. Note that all walls in contact with the liquid were made of glass to reduce the contamination. All experiments were conducted in a room with temperature control ($T=22\pm1$ °C).

Four types of silicone oil (polydimethylsiloxane) were used, purchased from Gelest Inc. Their properties, obtained from the manufacturer, are listed in Table I. The value of the Morton number, which is a "summary" of the fluid properties, is also shown. Note that the range of values of this number extends over four orders of magnitude. Although only the viscosity of the liquids was varied (the surface tension remained relatively constant), the combined effect of the variation of physical properties is representative of a wide range of common low-viscosity liquids. Results obtained with these liquids will systematically be compared to the reference data of Duineveld[3] obtained in hyperclean water. Also important are comparisons to the theoretical analysis of Moore,[14] who predicted the terminal velocity and aspect ratio of oblate spheroidal bubbles rising in straight line in the limit of very large Reynolds number. In particular, Moore calculated the bubble aspect ratio χ as a function of the Weber number We$=\rho U^2 d_{eq}/\sigma$ as if the fluid were *inviscid*. If we write the Weber number as a function of the other relevant dimensionless numbers for a *viscous* liquid, we have We $=\mathrm{Re}^2\mathrm{Mo}^{1/3}\mathrm{Ar}^{-2/3}$, where Re$=\rho d_{eq}U/\mu$ is the Reynolds number, Mo$=g\mu^4/(\rho\sigma^3)$ is the Morton number, and Ar $=\rho\sqrt{g d_{eq}^3}/\mu$ is the Archimedes number. Hence, assuming that Moore's prediction for the bubble shape still applies to bubbles rising in a viscous liquid provided Re is large enough, and considering that $\sigma_{oil}\approx\sigma_{water}/4$ according to Table I, a bubble rising in silicone oil will have the same aspect ratio (i.e., same We) as one rising in water provided the Reynolds number of the former is half that of the latter. This is of course only a rough estimate, since viscous effects also affect the bubble shape as will be shown below.

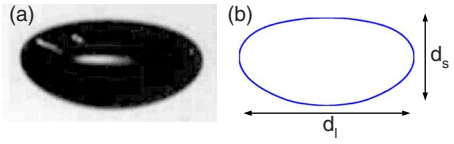

FIG. 1. (Color online) Typical bubble shape images obtained in DMS-T05 silicone oil with a bubble of $d_{eq}=2.64$ mm and $\chi=1.97$. (a) shows the original image and (b) shows the corresponding fit obtained through an expansion in Legendre polynomials. In (b) d_l and d_s are indicated.

To measure the shape and terminal velocity U of bubbles, a high speed camera was used (APX Photron). The images, as that shown in Fig. 1(a), were obtained at approximately 20 cm above the capillary to ensure that the bubbles had reached their terminal velocity. The optical array used in this study resulted in a resolution of around 35 pixels/mm, for an acquisition rate of 1000 frames/s. Using the MATLAB© Image Processing toolbox, the images were converted into binary format and the geometrical center of the blobs was located and tracked in time. With this routine, the equivalent diameter [$d_{eq}=(d_l^2 d_s)^{1/3}$, where d_l and d_s are the long and short bubble diameters, respectively] and the aspect ratio ($\chi=d_l/d_s$) was calculated for each case. A typical result is shown in Fig. 1(b). Also note that with our one-camera setup, it is not possible to precisely determine the bubble shape after the onset of the instability; hence, some experimental uncertainty is expected. Nevertheless, our study focuses on the determination of the critical conditions for which our setup is sufficient.

A series of typical images for increasing bubble sizes is shown in Fig. 2. For each experiment the bubble size was increased until the oscillating path was first detected. The conditions for transition were determined by interpolating the experimental conditions (d_{eq}, χ, U) in between the last straight and first oscillating paths. The critical conditions were identified using the bubble velocity. For bubbles below the transition, this velocity was nearly constant whereas once

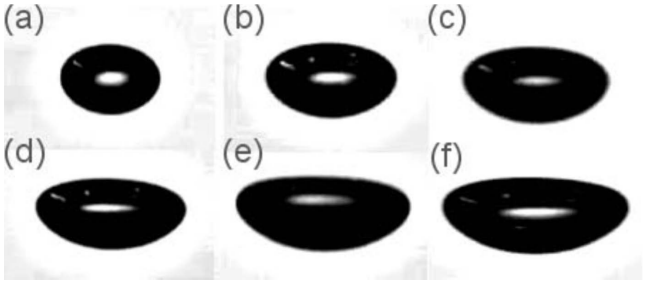

FIG. 2. Typical bubble images obtained in DMS-T02 silicone oil: (a) $d_{eq}=1.48$ mm, $\chi=1.64$; (b) $d_{eq}=2.06$ mm, $\chi=1.91$; (c) $d_{eq}=2.10$ mm, $\chi=1.99$; (d) $d_{eq}=2.33$ mm, $\chi=2.10$; (e) $d_{eq}=2.52$ mm, $\chi=2.43$; (f) $d_{eq}=2.60$ mm, $\chi=2.61$. Bubbles (a)–(c) have a straight path; (d) is the first bubble of the series to exhibit a zigzag path.

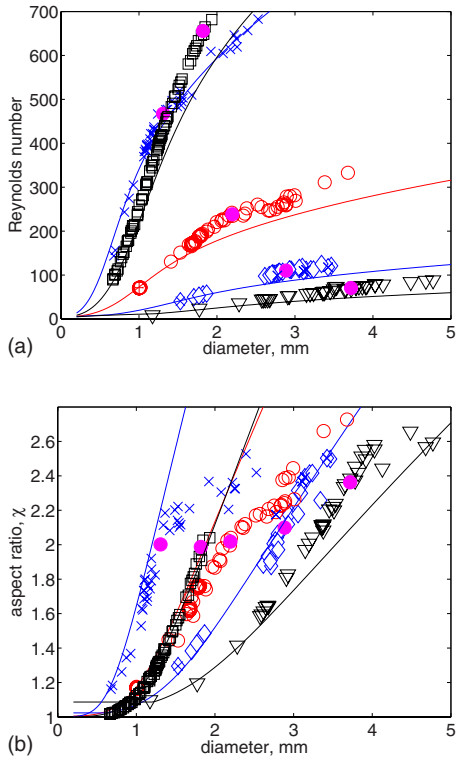

FIG. 3. (Color online) (a) Reynolds number Re as a function of the bubble equivalent diameter d_{eq}. (b) Bubble aspect ratio χ as a function of d_{eq}. Results for DMS-T00 (×), DMS-T02 (○), DMS-T05 (◇), DMS-T11 (▽); hyperclean water (□) (from Ref. 3). In (a), the solid lines show the prediction of Ref. 14; the error bars on the first data point of the DMS-T02 case show the magnitude of the experimental uncertainty (5%). The solid circles (●) show the critical conditions at which the transition to oscillatory path is detected.

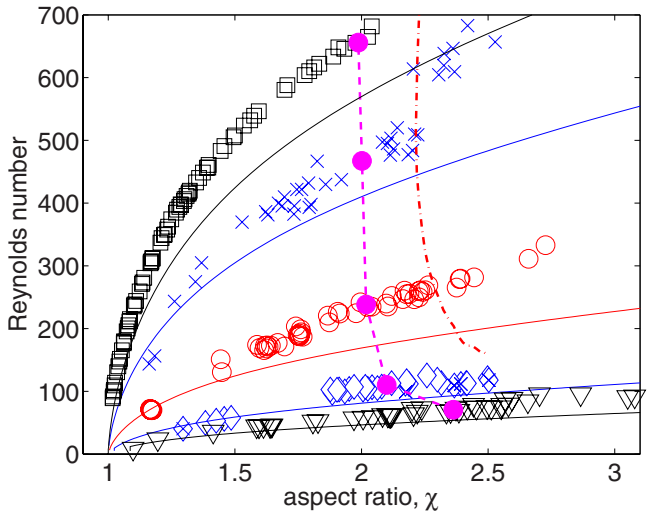

FIG. 4. (Color online) Reynolds number Re as a function of χ. All symbols are as in Fig. 3. The dashed line (that passes through the solid circles) shows the boundary of critical conditions; the dashed-dotted line shows the corresponding part of the critical curve reported by Ref. 11 for a fixed bubble.

the instability manifested itself, it fluctuated both in the vertical and horizontal directions. The bubble was considered to be above the transition point when the standard deviation of its velocity was larger that 5% of the terminal velocity. From the one-camera view it was not possible to determine whether the oscillatory path was a planar zigzag or a helix. Nevertheless, a few experiments were conducted by filming the bubble motion from above at incipient oscillating path for each liquid. In all cases, a zigzag type oscillation was observed.

Figure 3(a) shows the measured Reynolds number as a function of the equivalent bubble diameter. For all cases, the experimental Reynolds number is close to that predicted in Ref. 14. This is a clear indication that the assumption that the bubble surface is clean is correct. Note that the measured terminal velocities are slightly larger than those predicted in Ref. 14, a point also noted in Ref. 3. This discrepancy most likely results from the fact that the bubbles in the experiments are not perfect oblate spheroids, as shown in Fig. 2. For the case of the least viscous oil (DMS-T00), the terminal Reynolds number is very close to that found in water (from Ref. 3) for the same range of bubble diameters. The critical Reynolds number Re_c at which oscillations are first detected strongly decreases as the Morton number increases. This fact is at odds with what is known for the case of solid spheres where the wake first loses its axisymmetric structure at a well-defined Reynolds number.[15,16]

Figure 3(b) shows the measured aspect ratio χ as a function of the bubble size. As expected, the bubble becomes more oblate as its size increases, so that χ always increases with d_{eq}. For a given d_{eq}, χ also increases as surface tension decreases, i.e., from DMS-T11 to DMS-T00. However, surface tension changes by about 25% in between these two oils, whereas, in some range of d_{eq}, the aspect ratio is found to change by 70% for a given bubble diameter. This is a clear indication that the prediction of Ref. 14 for the bubble shape only provides a rough estimate under present experimental conditions. This is because viscous effects, which are not accounted for in this theory, significantly contribute to alter the bubble shape in the range of parameters we are considering. In other words, χ does not depend only on We but also on Re, as could be inferred from the fact that the problem has two independent control parameters, namely, We and Re (or Mo and Ar). The influence of these viscous effects is easily discernible in Fig. 2: Bubbles are becoming less fore-aft symmetric as their size increases, "large" bubbles being flatter at the front and more rounded at the back, owing to pressure corrections induced by viscous effects. Most notably, Fig. 3(b) indicates that the critical aspect ratio for which the transition to oscillatory behavior is first observed remains remarkably constant for "low-viscosity" oils (i.e., up to DMS-T05), increasing only for the most viscous oil. Note that the critical aspect ratio found for the low-viscosity oils is similar to that determined in Refs. 3 and 13 (i.e., $\chi \approx 2.0$) in hyperclean water.

Eliminating d_{eq} in between Figs. 3(a) and 3(b) allows us to obtain Fig. 4 which displays the evolution of Re as a function of χ. A similar plot was used in Ref. 11 to obtain the critical curve separating the regime where the wake of a fixed bubble is stable (i.e., axisymmetric) from that where it is fully three dimensional and thus produces a nonzero lift force. Here the region of stable rectilinear path lies to the left

of the dashed line. The results corresponding to transitional conditions indicate that Re_c changes drastically, falling from 467 for DMS-T00 to 70 for DMS-T11. With solid axisymmetric bodies, the configuration that yields the lowest Re_c is that of a flat solid disk moving broadside on, in which case Re_c is about 115.[15] Hence, when rising in a fluid of large enough viscosity, a spheroidal bubble may have a critical Re lower than any solid body. Combined with data available for hyperclean water which indicate $\mathrm{Re}_c \approx 650$,[3,13] present results show that the transition from straight to oscillatory path of spheroidal bubbles spans a full decade of Reynolds numbers. In contrast the aspect ratio only increases from 2.0 to 2.1 for the three least viscous oils, finally reaching 2.36 for TMS-T11. This is the key result of the present investigation. To figure out its significance, let us quickly come back to some of the conclusions reached in Ref. 11 for a fixed, perfectly spheroidal bubble. First it was shown there that, for large enough Re and χ, the normalized maximum vorticity $\omega_{\max} d_{\mathrm{eq}}/U$ at the bubble surface (reached at the equator of the bubble, where both the local fluid velocity and interface curvature are maximum) is independent of the Reynolds number and evolves as $\chi^{8/3}$. Then, when re-expressed in terms of surface vorticity, the critical curve separating the stable and unstable regions of the (χ, Re) phase space was shown to reduce to $\omega_{\max} d_{\mathrm{eq}}/U = 25 + 8.6 \times 10^{-3}$ Re. When applied to the present range of Re_c, this criterion, combined with the $\chi^{8/3}$-law, suggests that the critical aspect ratio should almost stay constant, varying by less than 5%. As shown by Fig. 4, this view is well supported by present results. The increase in the critical aspect ratio found with the most viscous oil can also be explained on the basis of the results of Ref. 11. Indeed, Fig. 5 of Ref. 11 shows that finite-Re effects still affect the strength of the surface vorticity for $\mathrm{Re} = O(10^2)$, $\omega_{\max}$ then decreasing significantly with decreasing Re. Typically, an oblate bubble with $\chi = 2.0$ and $\mathrm{Re} = O(10^3)$ is shown to produce as much vorticity as a bubble with $\chi = 2.35$ and $\mathrm{Re} = O(10^2)$. Therefore, to satisfy the above criterion, it is clear that a bubble rising with an $O(10^2)$ Reynolds number has to be slightly more oblate than its "high-Re" counterpart to generate the required amount of vorticity. Finally, the experimental results shown in Fig. 4 also indicate that the theoretical predictions of Ref. 11 for the critical aspect ratio are shifted by about 0.2 toward higher values. This difference can be explained on the basis of the fore-aft asymmetry of real bubbles in the transitional range, as compared to the perfect symmetry of the bubbles considered in Ref. 11. As real bubbles have flatter fronts than their perfectly spheroidal counterparts, the maximum curvature and surface fluid velocity which determine $\omega_{\max}$ have to be estimated from the geometry of their front half rather than from their overall aspect ratio. When re-evaluated in this way, the relevant aspect ratio χ_m is approximately 10% larger than $\chi = d_l/d_s$, as we defined from Fig. 1(b). For instance, the bubble in Fig. 1 corresponds to $\chi_m = 2.18$ rather than to $\chi = 1.97$. Using this correction, present results for freely moving bubbles are found to collapse on the theoretical predictions obtained in Ref. 11 with fixed bubbles. Additionally, some visualizations of the wake structure for bubbles after the instability were conducted: The presence of two counter-rotating streamwise vortices was observed, as previously reported experimentally,[9] in an indirect manner, and numerically.[2] These results will be presented elsewhere.

Therefore, combined with the numerical findings of Ref. 11, experimental results obtained with five different liquids now provide evidence of a one-to-one correspondence between the onset of the wake instability of a fixed bubble and that of the path instability of a freely moving bubble. Hence they confirm and extend the statement made in Ref. 8 on the basis of purely numerical results for perfectly oblate bubbles that there is a direct relationship between the instability of the bubble wake and that of its path. Moreover, they fully support the idea that the whole instability mechanism is governed by the amount of vorticity generated at the bubble surface, a process mostly related to the bubble oblateness.

These experiments were performed at IMFT during the sabbatical year of R.Z., who acknowledges the support of the PASPA program of UNAM. The technical assistance of S. Cazin was greatly appreciated.

[1] A. Prosperetti, C. Ohl, A. Tijink, G. Mougin, and J. Magnaudet, "Leonardo's paradox," J. Fluid Mech. **482**, 286 (2003).
[2] J. Magnaudet and I. Eames, "The motion of high-Reynolds-number bubbles in inhomogeneous flows," Annu. Rev. Fluid Mech. **32**, 659 (2000).
[3] P. C. Duineveld, "The rise of an ellipsoidal bubble in water at high Reynolds number," J. Fluid Mech. **292**, 325 (1995).
[4] R. Hartunian and W. Sears, "On the stability of small gas bubbles moving uniformly in various liquids," J. Fluid Mech. **3**, 27 (1957).
[5] T. B. Benjamin, "Hamiltonian theory for motion of bubbles in an infinite liquid," J. Fluid Mech. **181**, 349 (1987).
[6] D. I. Meiron, "On the stability of gas bubbles rising in inviscid fluid," J. Fluid Mech. **198**, 101 (1989).
[7] K. Ellingsen and F. Risso, "On the rise of an ellipsoidal bubble in water: oscillatory paths and liquid-induced velocity," J. Fluid Mech. **440**, 235 (2001).
[8] G. Mougin and J. Magnaudet, "Path instability of a rising bubble," Phys. Rev. Lett. **88**, 014502 (2002).
[9] A. de Vries, A. Biesheuvel, and L. van Wijngarden, "Notes on the path and wake of a gas bubble rising in pure water," Int. J. Multiphase Flow **28**, 1823 (2002).
[10] C. Brücker, "Structure and dynamics of the wake of bubbles and its relevance to bubble interaction," Phys. Fluids **11**, 1781 (1999).
[11] J. Magnaudet and G. Mougin, "Wake instability of a fixed spheroidal bubble," J. Fluid Mech. **572**, 311 (2007).
[12] B. Yang and A. Prosperetti, "Linear stability of the flow past a spheroidal bubble," J. Fluid Mech. **582**, 53 (2007).
[13] T. Sanada, M. Shirota, A. Sato, P. Stanovsky, J. Vejrazka, M. Ruzicka, and M. Watanabe, "A pair of bubbles in super purified water," in Sixth International Conference on Multiphase Flow, Leipzig, 2007 (ICMF, Leipzig, 2007), Paper No. S1-B-51.
[14] D. W. Moore, "The velocity of rise of distorted gas bubbles in a liquid of small viscosity," J. Fluid Mech. **23**, 749 (1965).
[15] R. Natarajan and A. Acrivos, "The instability of the steady flow past spheres and disks," J. Fluid Mech. **254**, 323 (1993).
[16] D. Ormieres and M. Provansal, "Transition to turbulence in the wake of a sphere," Phys. Rev. Lett. **83**, 80 (1999).